International Journal for Advanced Research

Journal homepage: https://journal.outlinepublisher.com/index.php/ijar

Research Article

Magnetohydrodynamic Nanofluid Flows Over a Smart Fabric Under the Effects of Mixed Convection, Magnetic Field, Stretching Force, and Radiation

Zaitun [1]* , Widodo B [2], Imron C [3] , Adzkiya D [4]

[1]Science Department Institut Teknologi Bacharuddin Jusuf Habibie Parepare, Indonesia
[2,3,4] Mathematics Department Institut Teknologi Sepuluh Nopember Surabaya, Indonesia

*Correspondence: E-mail: zaitun.zt99@ith.ac.id

Keywords:
Magnetohydrodynamic,
Nanofluid,
Smart Fabric,
Radiative Flux.

Abstract

The study of Magnetohydrodynamic (MHD) has been widely discussed with complex problems. Just as this topic involves inductive polymers or smart fabrics for engineering in machinery or protective equipment. The smart fabrics that can be involved in MHD studies become a useful material. The smart fabric is a sheet of inductive polymer that can be an influence in the MHD analysis as well as a parameter that can be considered. In this study, the MHD of nanofluid, namely Iron-(III)-oxide flows past in smart fabrics under influence of magnetic field and radiative flux is studied by constructing a mathematical model and then the model solved numerically using the Keller-Box scheme. The effect of Mixed Convection and stretching parameter is considered on the model. Numerical simulations were carried out to examine the effect of the parameters, are obtained the profile of velocity and temperature increase when the magnetic and stretching parameters increases, the velocity profile and temperature decreases when the Prandtl number are increases, the profiles of velocity are decreases and temperature increases when porosity variable and volume fraction parameter's value increases, and the profile of temperature increase when the mixed convection's value and the radiation parameter increases.

Introduction

Various phenomena in nature both in the fields of chemistry, biology, and physics can be made by mathematical models (Zaitun et al., 2021). In the analysis, the theory that needs to be used to support the proof that a mathematical equation represents the phenomenon. In the phenomenon of mass transfer or heat transfer, for example, a mathematical model of fluid flow can then be formed (Zaitun et al., 2024; Manvi et al., 2022). In fluid flow, it is necessary to carry out a basic analysis of the model formation and its solution. Fluid flow models such as type fluid or flow on influence built through continuity equations, mass conservation equations, energy equations, and several supporting theories can form a mathematical model that represents fluid phenomena which can then be called type fluids or magnetohydrodynamics.

Magnetohydrodynamic (MHD) is studied about the relation of fluid flow and magnetic fields (Kumar et al., 2025; Reddy & Goud, 2022; Widodo et al., 2020). Magnetohydrodynamics is a magnetic field that can induce an electric in a moving conductive liquid, which in turn polarizes the liquid and reciprocally changes the magnetic field itself (Sheikholeslami Kandelousi, 2017; Widodo, 2021; Mayagrafinda & Widodo, 2022; Mardianto et al., 2020; Norasia et al., 2021; Widodo et al., 2015; Rumite et al., 2015; Widodo et al., 2015; Yasin et al., 2021). Magnetohydrodynamics is important in generator applications with engineering and industrial applications such as magnetohydrodynamics, nuclear reactor reactors, crystallization of ship propulsion engines, manufacture of type protective polymer materials (Widodo, 2021; Kumar & Reddy, 2023).

Fluids that can be induced by electric current and are conductive are mixed fluids such as molten metal, plasma (ionized gas), and strong electrolyte fluids (Jamrus et al., 2025; Khashi'ie et al., 2022; Jeelani & Abbas, 2025). Liquids such as molten metal have metal particles whose size is so small that they are commonly called nanofluids (nanofluids). Nanofluids are liquids or solutions containing nano-sized particles, which have a very small size of 1-100 nm which can also be present in basic fluids such as water (Mohammadein et al., 2018; Nandi et al., 2022; Rafique et al., 2025). Nano effect fluid with the aim of being able to play a role in the performance of the fluid, so that the addition of these particles can be useful as a catalyst in terms of temperature or vice versa, increasing the surface heat transfer that occurs and the heat transfer that occurs (Norasia et al., 2021). The use of liquid metals or nanofluids in the case of MHD, has been widely developed such as Ferrofluid, Lithium, Iron or Aluminum Mixtures, and so on. The media or objects studied in the fluid flow that pass through it have also been carried out by several researchers, such as solid sphere by (Mardianto et al., 2020; Norasia et al., 2021; Rumite et al., 2015; Yasin et al., 2021), porous cylinder by (Widodo et al., 2015; Ellahi et al., 2011; Widodo et al., 2015), Sliced ball by (Widodo, 2021; Nursalim et al., n.d.), porous sliced ball in (Widodo et al., 2020), and the stretched sheet or the plate (Alizadeh-Pahlavan & Borjian-Boroujeni, 2008; Chaudhary & Kumar, 2014; Nield & Kuznetsov, 2003; Pantzali et al., 2009; Zainal et al., 2020).

The focus of this research is on the stagnation point $y \approx 0$ of the boundary layer formed from a fluid flow that moves vertically from bottom to top through the surface of an inductive polymer or smart fabric, then using various concepts of the laws of physics. Then we can build continuity equations, momentum equations, and energy equations. In the method section, the Keller-box scheme of numerical method is used, which is an implicit numerical method for the mathematical model of magnetohydrodynamics in a boundary layer flowing through a vertically stretched smart fabric under the influence of a magnetic field and radiation flux. Investigations for parameter variations were carried out on numerical simulations and their analysis for variations of several parameters on velocity and temperature profile.

Mathematical Model

Several assumptions were made, the nanofluid flowing at a constant velocity U_∞ and constant temperature T_∞ in a magnetic field space, initially not magnetized but after the surface of the conductive polymer is stretched vertically upwards with velocity in the wall is $U_w(x) = \left(U_\infty \left(c\nu_f\right)\right)^{\frac{1}{2}x}$, a magnetic induction event occurs, so that the fluid initially not magnetized, after passing through the magnetic field around the surface of the smart fabrics becomes magnetically charged. (Fatunmbi & Adeniyan, 2020; Swain et al., 2023). The focus of this research is at the stagnation point $y \approx 0$ of the boundary layer which is formed from a fluid flow that moves vertically from bottom to top through the surface of a smart fabric, then various concepts of the laws of physics are used (Wajeeha et al., 2024). From these laws, the continuity equations, momentum equations, and energy equations can be formed. To construct the model of the problem, briefly the illustration of smart fabrics is shown by the figure where the smart fabrics is vertical stretched by a force.

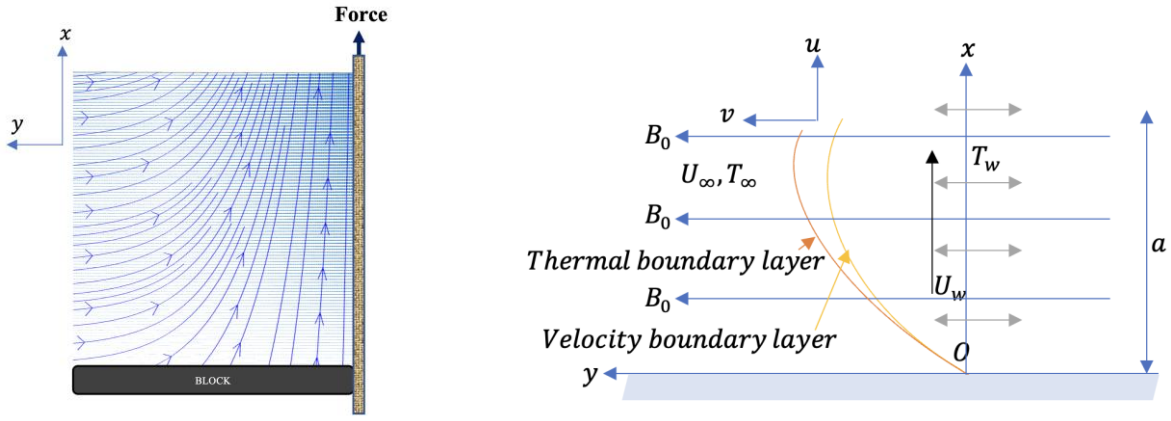

(a) (b)

Figure 1
Illustration of the smart fabrics (a) and the coordinates systems (b)

The form of mathematical model that represents magnetohydrodynamics phenomena. We consider the dimensional mathematical model as:

Continuity equation

$$\frac{\partial \underline{u}}{\partial \underline{x}} + \frac{\partial \underline{v}}{\partial \underline{y}} = 0 \tag{1}$$

Momentum equation

$$\rho_{fn}\left(\underline{u}\frac{\partial \underline{u}}{\partial \underline{x}} + \underline{v}\frac{\partial \underline{u}}{\partial \underline{y}}\right) = \mu_{fn}\frac{\partial^2 \underline{u}}{\partial \underline{y}^2} - \left(\sigma B_0^2 - \frac{\mu_{fn}}{K}\right)\underline{u} + g_{\underline{x}}\beta(\underline{T} - T_\infty). \tag{2}$$

Energy equation

$$\rho c_p\left(\underline{u}\frac{\partial \underline{T}}{\partial \underline{x}} + \underline{v}\frac{\partial \underline{T}}{\partial \underline{y}}\right) = k\left(\frac{\partial^2 \underline{T}}{\partial \underline{x}^2} + \frac{\partial^2 \underline{T}}{\partial \underline{y}^2}\right) + \frac{16\sigma^* T_\infty^3}{3k^*}\left(\frac{\partial^2 \underline{T}}{\partial \underline{x}^2} + \frac{\partial^2 \underline{T}}{\partial \underline{y}^2}\right) \tag{3}$$

where the boundary condition in dimensional
$\underline{u} = 0, \underline{v} = 0, \underline{T} = T_w$, for $\underline{x} = 0$
$\underline{u} = U_\infty, \underline{v} \to 0, \underline{T} = T_\infty$, for $\underline{x} \to \infty$.
The previous mathematical form is dimensional equation, so we have to transform the form to dimensionless equations with non-dimensional parameters (Widodo, 2021). The parameters non-dimensional is:

$$x = \frac{\underline{x}}{a}, y = \frac{Re^{\frac{1}{2}}\underline{y}}{a}, u = \frac{\underline{u}}{U_\infty}, v = \frac{Re^{\frac{1}{2}}\underline{v}}{U_\infty}, Re = \frac{U_\infty a}{\nu_{fn}}, \nu_{fn} = \frac{\mu_{fn}}{\rho_{fn}}, g = \frac{g_{\underline{x}}}{cU_\infty}, \text{dan } \theta = \frac{\underline{T} - T_\infty}{T_w - T_\infty}$$

then the Energy Equation is

$$u\frac{\partial \theta}{\partial x} + v\frac{\partial \theta}{\partial y} = \frac{\zeta^*}{Pr}\varrho\left(\kappa + \frac{4}{3}Rn\right)\left(\frac{\partial^2 \theta}{\partial x^2} + Re\frac{\partial^2 \theta}{\partial y^2}\right) \tag{5}$$

with magnetic parameter $M = \frac{a\sigma B_0^2}{U_\infty \rho_{fn}}$, porosity parameter $\phi = \frac{a\mu_{fn}}{U_\infty \rho_{fn} K}$, Prandtl number $Pr = \frac{\nu_{fn}(\rho C_p)_f}{k_f}$, density ratio $\varrho = \frac{(\rho C_p)_f}{(\rho C_p)_{fn}}$, thermal conductivity $\kappa = \frac{k_{fn}}{k_f}$, and radiation parameter $Rn = \frac{4\sigma^* T_\infty^3}{k^* k_f}$ and constant $\zeta^* = \frac{1}{aU_\infty}$, $\omega^* = \frac{gca\beta(T_w - T_\infty)}{U_\infty \rho_{fn}}$
where the boundary condition in non-dimensional equation
$u = 0, \quad T = T_w$, for $x = 0$
$u = U_\infty \quad T = T_\infty$, for $x \to \infty$
The non-dimensional from Equation (4)-(5) then these equations are converted into a similarity equation using the stream function. This is because the nonlinear system of partial differential equations is to be transformed into a nonlinear system of ordinary differential equations (Sheikholeslami, Kandelousi, 2017; Beg, 2014). Then it is easier to solve numerically by similarity equation

$$\psi = U_\infty(c\nu_f)^{\frac{1}{2}} a y f(\eta), \qquad \eta = \left(\frac{c}{\nu_f}\right)^{\frac{1}{2}} ax, \qquad u = \frac{\partial \psi}{\partial y}, \qquad v = -\frac{\partial \psi}{\partial x}$$

With the mixed convection parameter $\gamma = \frac{Gr}{Re^2}$, $\lambda = \frac{\gamma}{ca^2\nu_f\left(\frac{c}{\nu_f}\right)^{\frac{1}{2}}}$, Parameter $\vartheta = \frac{1}{U_\infty c^2 a}$, and constant $\zeta = \frac{\zeta^*}{U_\infty ca} = \frac{1}{U_\infty{}^2 ca^2}$ to

momentum equation will be

$$ff' = \frac{\nu_{nf}}{\nu_f}\zeta f'' - (M - \phi)\vartheta f + \lambda\theta \tag{6}$$

and the energy equation is

$$f\theta' - \lambda\frac{1}{Pr}\varrho\left(\kappa + \frac{4}{3}Rn\right)\theta'' = 0 \tag{7}$$

for the several parameters, we use approximation of kinematic viscosity ratio, the density and the ratio of thermal conductivity (Widodo, 2021) for χ is volume fraction parameter

$$\rho_{fn} = (1-\chi)\rho_f + \chi\rho_s$$

$$\mu_{fn} = \frac{\mu_f}{(1-\chi)^{2.5}}$$

$$(\rho C_p)_{fn} = (1-\chi)(\rho C_p)_f + \chi(\rho C_p)_s$$

$$\frac{k_{fn}}{k_f} = \frac{(k_s + k_f) - 2\chi(k_f - k_s)}{(k_s + 2k_f) + \chi(k_f - k_s)}$$

$$\frac{\nu_{nf}}{\nu_f} = \frac{1}{(1-\chi)^{2.5}\left((1-\chi) + \chi\left(\frac{\rho_s}{\rho_f}\right)\right)}$$

for the boundary condition for similarity equation
$f(\eta) = 0, f'(\eta) = 1, \theta(\eta) = 1, \eta = 0$
$f'(\eta) = 0, \quad \theta(\eta) = 0, \eta \to \infty$

Method

To understand and solve this problem, a mathematical model was constructed. This mathematical model is built using the principles of conservation of mass, momentum, energy, and Maxwell's equations. From these Maxwell's principles and equations, the dimensional governing equations for continuity, momentum, and energy of nanofluids are obtained. These dimensional governing equations are then transformed into dimensionless governing equations using the appropriate dimensionless variables (Widodo et al., 2015). Furthermore, the stream function is introduced to express a function that represents the flow velocity and fluid temperature (Widodo et al., 2020). Then, similarity variables are used to reduce the non-dimensional governing equations into a system of nonlinear differential equations. The system of nonlinear differential equations is then solved numerically using the Keller-Box implicit numerical scheme (Prasad et al., 2014). From this numerical solution/simulation, the effect of radiation, mixed convection, porosity, strain, Prandtl number and magnetic field is analyzed on changes in flow velocity and fluid temperature on the surface of the smart fabric.

Results and Discussion

Before simulation the thermophysical properties of water and iron-(III)-oxide (Fe2O3) are given in Table 1. In the analysis, the similarity equation has been solved and the results are shown in this section. The several parameters are also considered by different values and these results have been made at fixed values for every parameter except for parameters of that variety.

Table 1

Thermo-physical properties of water and iron-(III)-oxide (Fe2O3) (Tawade et al., 2022; Takeda et al., 2009; Waqas et al., 2016; Minea, 2019; Kumar et al., 2025).

Parameter	Water	Fe_2O_3
Density (kg/m^3)	997.1	5260

Thermal Conductivity (W/mK)	0.613	0.58
Specific Heat (j/kgK)	4179	103.9
$\beta \times 10^5\ (K^{-1})$	21	1.25
Electrical conductivity (σ)	0.05	2700

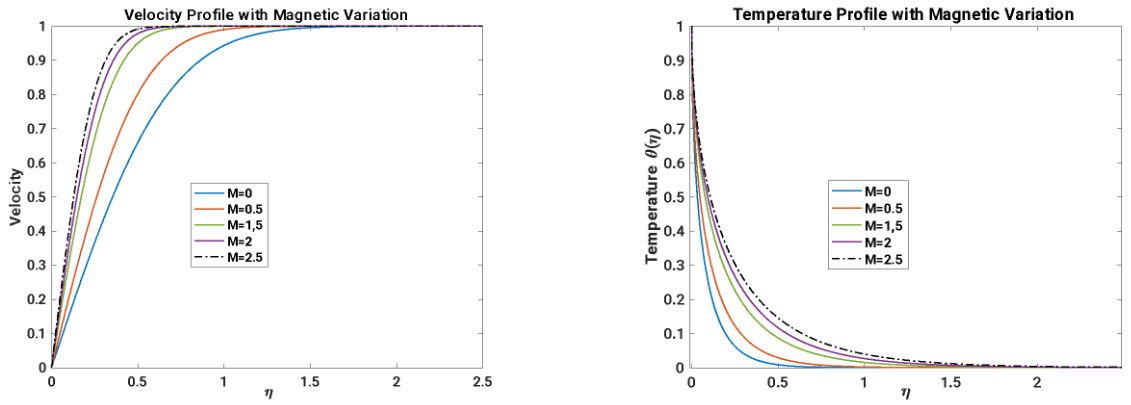

(a) (b)

Figure 2
Graph of velocity profile (a) and Temperature (b) for the Magnetic parameter is variety.

For variation of magnetic parameters $M = 0, M = 0.5, M = 1.5, M = 2.5$, and $M = 2$, it can be seen in Figure 2 that with increasing magnetic parameter value, the velocity profile increases and the temperature value profile also increases. This situation occurs because as the magnetic field parameter increases, the magnetic field in the area increases as a result, the greater the magnetic parameter is cause greater the attractiveness of the smart fabrics to the fluid. For the temperature profile is caused by the influence of particle friction, namely the occurrence of nanoparticle collisions so that the fluid temperature increases with increasing magnetic parameter.

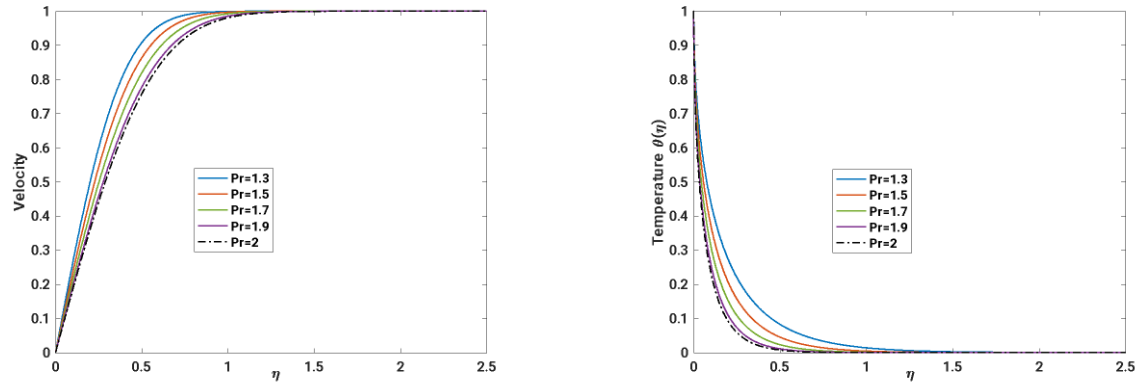

(a) (b)

Figure 3
Graph of velocity profile (a) and Temperature (b) for the Prandtl Number is variety

For variation of Prandtl Number $Pr = 1.3, Pr = 1.5, Pr = 1.7, Pr = 1.9$, and $Pr = 2$, it can be seen in Figure 3 that with increasing Prandtl Number value, the velocity profile are decreases and the temperature value profile also decreases, because the Prandtl number is inversely proportional to the thermal diffusivity parameter and directly proportional to the kinematic viscosity. Therefore, the greater the Prandtl number, the greater the value of the kinematic viscosity of the fluid so that the viscosity of the fluid increases. This means that the greater the Prandtl number, the velocity and temperature profile decreases.

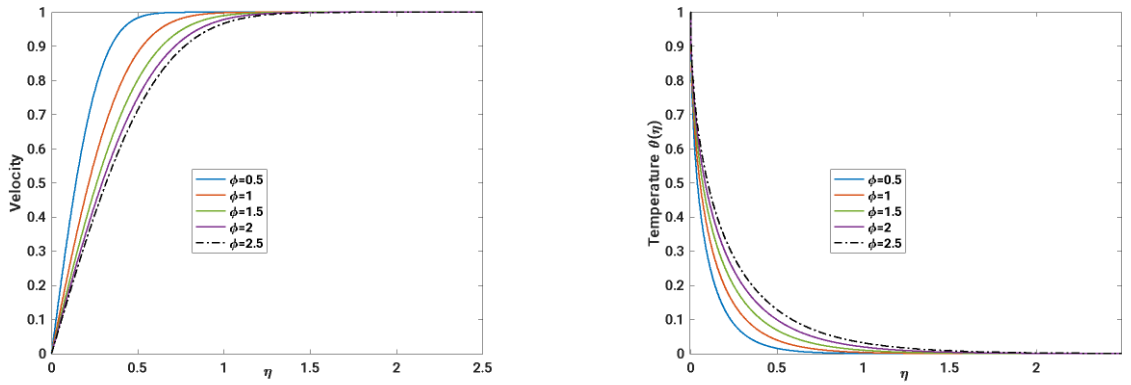

(a) (b)

Figure 4
Graph of velocity profile (a) and Temperature (b) for the Porosity parameter is variety

For variation of Porosity parameters $\phi = 0.5, \phi = 1, \phi = 1.5, \phi = 2$, and $\phi = 2.5$, it can be seen in Figure 4 that with increasing porosity parameter value, the velocity profile increases and the temperature value profile also increases. This situation occurs because the porosity parameter is directly proportional to the dynamic viscosity of the nanofluid and inversely proportional to the density of the nanofluid. Then according to the Darcy model that was previously introduced, the porosity parameter is related to the permeability value or to the relationship between permeability and velocity, namely the greater the permeability value, the lower the velocity value. On the temperature profile due to the increased level of viscosity resulting in increased friction.

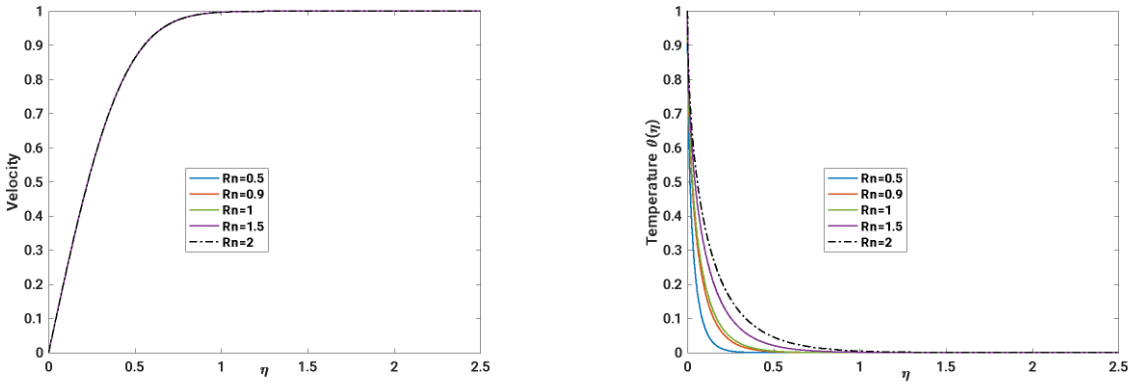

(a) (b)

Figure 5
Graph of temperature for the Radiation parameter is variety

For variation of radiation parameters $Rn = 0.5, Rn = 0.9, Rn = 1, Rn = 1.5$, and $Rn = 2$ It can be seen in Figure 5 that with increasing radiation parameter value, the velocity profile does not change and the temperature value profile also increases. The radiative parameter is the dominant level relation of the heat source, if the radiative parameter is large, the heat source is more dominant by the influence of radiation and vice versa if the radiation parameter is small, the heat source is more dominant than the conductivity of the medium. The conductivity property is not directly related to the viscosity level of the fluid, but it does not mean that it affects the friction level and fluid velocity because the radiation parameter only gives the level of dominance of the heat source so that it directly affects the temperature value.

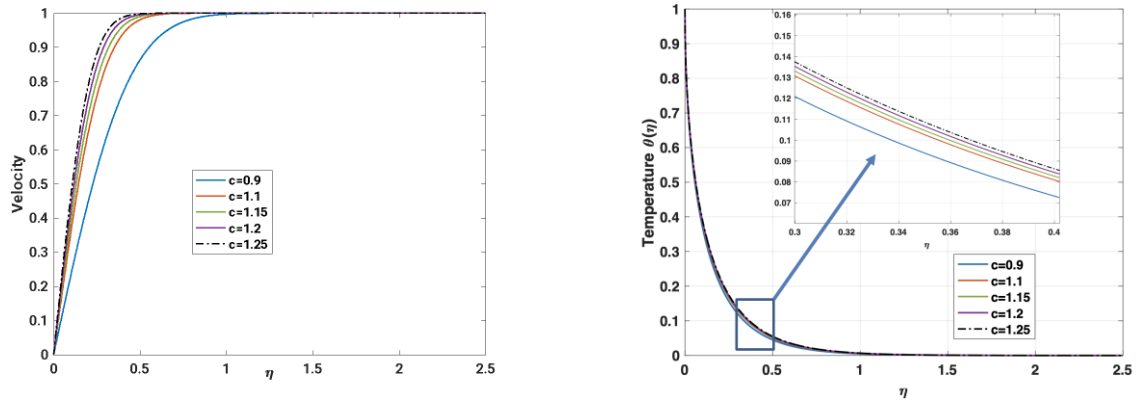

(a) (b)

Figure 6

Graph of velocity profile (a) and Temperature (b) for the Stretching Parameter is variety

For variation of Stretching parameters $c = 0.9, c = 1.1, c = 1.15, c = 1.2$, and $c = 1.25$, It can be seen in Figure 6 that with increasing Stretching parameter value, the velocity profile increases and the temperature value profile also increases. This situation occurs because the stretching properties of the fabric sheet cause the velocity value at the boundary layer to increase due to the strain properties which are directly proportional to the velocity of the fabric sheet. The strain properties are also identical to the porosity properties so that the simulation results also have the same effect on the velocity and temperature profiles. So that the graph of the relationship between the strain parameter with the velocity and temperature profile is a straight comparison with the properties of the porosity parameter.

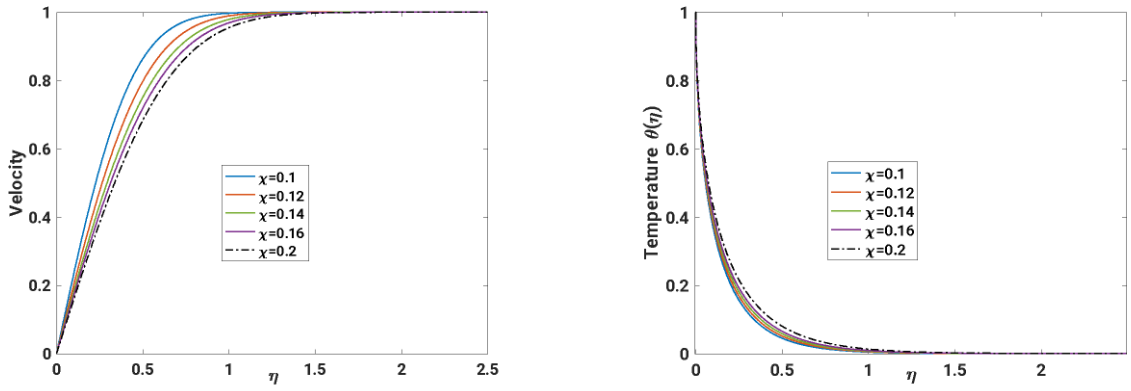

Figure 7

Graph of velocity profile (a) and Temperature (b) for the Volume Fraction Parameter is variety

For variation of volume fraction parameters $\chi = 0.1, \chi = 0.12, \chi = 1.14, \chi = 0.16$, and $\chi = 0.2$ It can be seen in Figure 7 that with increasing volume fraction parameter value, the velocity profile increases and the temperature value profile also increases, because the volume fraction is related to the nature of the mixture of nanofluids and base fluids. These properties affect the viscosity of nanofluids so that if the viscosity of the fluid is greater, the friction level on the cloth sheet will be greater, resulting in a decrease in the velocity value and the frictional properties also result in an increase in energy or an increase in temperature for the volume fraction parameter value which also increases.

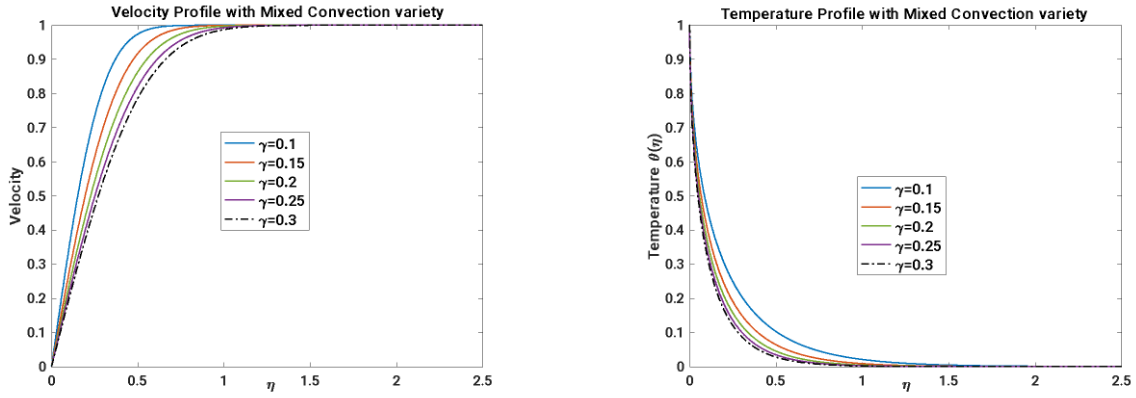

(a) (b)

Figure 8
Graph of velocity profile (a) and temperature (b) for the mixed convection parameter is variety

For variation of mixed convection parameters $\gamma = 0.1, \gamma = 0.15, \gamma = 0.2, \gamma = 0.25$, and $\gamma = 0.3$, by Figure 8 it is shown that with increasing mixed convection parameter value, the velocity profile increases and the temperature value profile also increases. This situation occurs because the location of the heat source is close to the stagnation point so the density decreases and velocity increases. The temperature profile increase is caused by the Grashof Number increases in λ parameter and it causes the viscosity to decrease and the temperature profile increases.

Conclusion

The numerical results from the Keller-Box scheme provide detailed insights into the behavior of iron (III)-oxide water-based nanofluid flow over stretched smart fabrics under the influence of magnetic fields and radiation. The increase in both velocity and temperature profiles with the magnetic parameter (M) reflects the presence of Lorentz forces in magnetohydrodynamic (MHD) flows. These forces accelerate the fluid and simultaneously introduce resistive (Joule) heating, raising the temperature. Similarly, the stretching parameter (c) intensifies the fluid motion due to enhanced tangential stress on the surface, leading to increased velocity and frictional heating, which also elevates the temperature. An increase in the radiation parameter (Rn) contributes to greater radiative heat transfer, resulting in a higher temperature profile consistent with radiative transport theory.

The Prandtl number (Pr) plays a crucial role in governing thermal diffusivity relative to momentum diffusivity. As Pr increases, the thermal boundary layer becomes thinner, leading to a reduction in both the temperature and velocity profiles due to weaker buoyancy forces and reduced heat conduction. The porosity parameter (ϕ) influences the flow resistance in the medium; as it increases, fluid motion is impeded, resulting in a decrease in velocity. However, reduced convective heat transport causes greater heat accumulation near the surface, which increases the temperature profile. Similarly, an increase in the volume fraction of nanoparticles (χ) raises the effective thermal conductivity of the fluid, enhancing heat transfer but increasing viscosity and density, which dampens the velocity.

Furthermore, the mixed convection parameter (γ), which represents the ratio of buoyancy-driven to force-driven flow, enhances both the velocity and temperature profiles when increased. This reflects the combined effects of natural and forced convection, where buoyancy augments fluid motion and improves thermal energy distribution. Overall, the simulation results are consistent with established theories in MHD, porous media flow, and nanofluid thermophysics. These findings offer valuable guidance for optimizing smart textile applications where controlled heat and fluid flow behavior are critical, particularly in environments where external fields and material stretching are involved.

References

Alizadeh-Pahlavan, A., & Borjian-Boroujeni, S. (2008). On the analytical solution of viscous fluid flow past a flat plate. *Physics Letters, Section A: General, Atomic and Solid State Physics*, *372*(20), 3678-3682. 10.1016/j.physleta.2008.02.050

Beg, O. A. (2014). Homotopy Analysis of Magnetohydrodynamic Convection Flow in Manufacture of a Viscoelastic Fabric for Space Applications. *Int. J. of Appl. Math and Mech*, *10*(10), 9-49. https://www.researchgate.net/publication/268512624

Chaudhary, S., & Kumar, P. (2014). MHD forced convection boundary layer flow with a flat plate and porous substrate. *Meccanica*, *49*(1), 69-77. 10.1007/s11012-013-9773-0

Ellahi, R., Zeeshan, A., Vafai, K., & Rahman, H. U. (2011). Series solutions for magnetohydrodynamic flow of non-Newtonian nanofluid and heat transfer in coaxial porous cylinder with slip conditions. *Proceedings of the Institution of Mechanical Engineers, Part N: Journal of Nanoengineering and Nanosystems*, *225*(3), 123-132. 10.1177/1740349911429759

Fatunmbi, E. O., & Adeniyan, A. (2020). Nonlinear thermal radiation and entropy generation on steady flow of magneto-micropolar fluid passing a stretchable sheet with variable properties. *Results in Engineering*, *6*, 100142. 10.1016/j.rineng.2020.100142

Jamrus, F. N., Waini, I., Khan, U., & Ishak, A. (2025). Stagnation slip flow of ternary hybrid nanofluid over an exponentially shrinking/Stretching sheet with joule heating, MHD, and thermal radiation effects. *Chinese Journal of Physics*, *94*, 518-539. 10.1016/j.cjph.2025.01.042

Jeelani, M. B., & Abbas, A. (2025). Energy transport in MHD Maxwell hybrid nanofluid flow over inclined stretching porous sheet with effects of chemical reaction, solar radiation and porous medium. *Case Studies in Thermal Engineering*, *68*, 105915. 10.1016/j.csite.2025.105915

Khashi'ie, N. S., Waini, I., Kasim, A. R. M., Zainal, N. A., Ishak, A., & Pop, I. (2022). Magnetohydrodynamic and viscous dissipation effects on radiative heat transfer of non-Newtonian fluid flow past a nonlinearly shrinking sheet: Reiner–Philippoff model. *Alexandria Engineering Journal*, *61*(10), 7605-7617. 10.1016/j.aej.2022.01.014

Kumar, L., Singh, A., Joshi, V. K., & Sharma, K. (2025). MHD micropolar fluid flow with hall current over a permeable stretching sheet under the impact of Dufour-Soret and chemical reaction. *International Journal of Thermofluids*, *26*, 101042. 10.1016/j.ijft.2024.101042

Kumar, M. A., & Reddy, Y. D. (2023). Computational modelling of radiative Maxwell fluid flow over a stretching sheet containing nanoparticles with chemical reaction. *Journal of the Indian Chemical Society*, *100*(1), 100877. 10.1016/j.jics.2022.100877

Kumar, S., Choudhary, S., Kumari, K., Sharma, A., & Choudhary, P. (2025). MHD darcy-forchheimer flow of SWCNT-H2O nanofluid over a porous stretching sheet. *International Journal of Thermofluids*, *26*, 101064. 10.1016/j.ijft.2025.101064

Manvi, B., Tawade, J., Biradar, M., Noeiaghdam, S., Fernandez-Gamiz, U., & Govindan, V. (2022). The effects of MHD radiating and non-uniform heat source/sink with heating on the momentum and heat transfer of Eyring-Powell fluid over a stretching. *Results in Engineering*, *14*, 100435. 10.1016/j.rineng.2022.100435

Mardianto, L., Widodo, B., & Adzkiya, D. (2020). Aliran Konveksi Campuran Magnetohidrodinamik yang Melewati Bola Bermagnet. *Limits: Journal of Mathematics and Its Applications*, *17*(1), 9. 10.12962/limits.v17i1.6752

Mayagrafinda, I., & Widodo, B. (2022). Magnetohidrodinamika Fluida Nano yang Melalui Silinder Vertikal Berpori. *J. Ris. & Ap. Mat*, *06*(1), 31-39.

Minea, A. A. (2019). A review on electrical conductivity of nanoparticle-enhanced fluids. *Nanomaterials*, *9*(11). 10.3390/nano9111592

Mohammadein, S. A., Raslan, K., Abdel-Wahed, M. S., & Abedel-Aal, E. M. (2018). KKL-model of MHD CuO-nanofluid flow over a stagnation point stretching sheet with nonlinear thermal radiation and suction/injection. *Results in Physics*, *10*, 194-199. 10.1016/j.rinp.2018.05.032

Nandi, S., Kumbhakar, B., & Sarkar, S. (2022). MHD stagnation point flow of Fe3O4/Cu/Ag-CH3OH nanofluid along a convectively heated stretching sheet with partial slip and activation energy: Numerical and statistical approach. *International Communications in Heat and Mass Transfer*, *130*. 10.1016/j.icheatmasstransfer.2021.105791

Nield, D. A., & Kuznetsov, A. V. (2003). Boundary-layer analysis of forced convection with a plate and porous substrate. *Acta Mechanica*, *166*(1-4), 141-148. 10.1007/s00707-003-0050-5

Norasia, Y., Widodo, B., & Adzkiya, D. (2021). Pergerakan Aliran MHD Ag-AIR Melewati Bola Pejal. *Limits: Journal of Mathematics and Its Applications*, *18*(1), 15. 10.12962/limits.v18i1.7888

Nursalim, R., Widodo, B., & Imron, C. (n.d.). Magnetohydrodynamics of unsteady viscous fluid on boundary layer past a sliced sphere. *Journal of Physics: Conference Series*, *893*(1). 10.1088/1742-6596/893/1/012044

Pantzali, M. N., Kanaris, A. G., Antoniadis, K. D., Mouza, A. A., & Paras, S. V. (2009). Effect of nanofluids on the performance of a miniature plate heat exchanger with modulated surface. *International Journal of Heat and Fluid Flow*, *30*(4), 691-699. 10.1016/j.ijheatfluidflow.2009.02.005.

Prasad, K. V., Kuppalapalle, & Vajravelu. (2014). Keller-Box Method and Its Application. *De Gruyter*.

Rafique, K., Asim, A., Alshehery, S., Younas, B., Khan, I., & Khan, M. S. (2025). Thermal radiation and stability aanalysis in dual solutions of Al2O3-Cu/H2O hybrid nanofluid flow over a stretching/shrinking surface with arrhenius kinetic energy. *Journal of Radiation Research and Applied Sciences*, *18*(2), 101510. 101510; 10.1016/j.jrras.2025.101510

Reddy, Y. D., & Goud, B. S. (2022). MHD heat and mass transfer stagnation point nanofluid flow along a stretching sheet influenced by thermal radiation(Article). *Journal of Thermal Analysis and Calorimetry*, *147*(21), 11991-12003. 10.1007/s10973-022-11430-4

Rumite, W., Widodo, B., & Imron, C. (2015). The Numerical Solution of Free Convection Flow of Viscoelastic Fluid Past Over a Sphere. *Proceeding of International Conference On Research, Implementation And Education Of Mathematics And Sciences*, 109-116.

Sheikholeslami Kandelousi, M. (2017). *Nanofluid Heat and Mass Transfer in Engineering Problems* (M. Sheikholeslami Kandelousi, Ed.). IntechOpen. 10.5772/65803

Swain, K., Ibrahim, S. M., Dharmaiah, G., & Noeiaghdam, S. (2023). Numerical study of nanoparticles aggregation on radiative 3D flow of maxwell fluid over a permeable stretching surface with thermal radiation and heat source/sink. *Results in Engineering*, *19*, 101208. 10.1016/j.rineng.2023.101208

Takeda, M., Onishi, T., Nakakubo, S., & Fujimoto, S. (2009). Physical properties of iron-oxide scales on Si-containing steels at high temperature. *Materials Transactions*, *50*(9), 2242-2246. 10.2320/matertrans.M2009097

Tawade, J. V., Guled, C. N., Noeiaghdam, S., Fernandez-Gamiz, U., Govindan, V., & Balamuralitharan, S. (2022). Effects of thermophoresis and Brownian motion for thermal and chemically reacting Casson nanofluid flow over a linearly stretching sheet. *Results in Engineering*, *15*, 100448. 10.1016/j.rineng.2022.100448

Wajeeha, K., Sushma, M. N., Mahabaleshwar, U. S., Mahesh, R., & Yadav, D. (2024). The Effect of Casson Fluid Flow on a Stagnation Point Over a Porous Stretching Sheet with Thermal Radiation. *Heat Transfer Enhancement Techniques: Thermal Performance, Optimization and Applications*, *17*. 10.1002/9781394270996.ch17

Waqas, M., Farooq, M., Khan, M. I., Alsaedi, A., Hayat, T., & Yasmeen, T. (2016). Magnetohydrodynamic (MHD) mixed convection flow of micropolar liquid due to nonlinear stretched sheet with convective condition. *International Journal of Heat and Mass Transfer*, *102*, 766-772. 10.1016/j.ijheatmasstransfer.2016.05.14

Widodo, B. (2021). Magnetohydrodynamics fluid flow passing through a sliced magnetic sphere influenced by mixed convection. *Journal of Physics*, *1836*(1). 10.1088/1742-6596/1836/1/012042

Widodo, B., Imron, C., Asiyah, N., Siswono, G. O., Rahayuningsih, T., & Purbandini. (2015). Viscoelastic Fluid Flow Pass a Porous Circular Cylinder When the Magnetic Field Included. *Far East Journal of Mathematical Sciences (FJMS)*, *99*(2), 173-186. 10.17654/MS099020173

Widodo, B., Nugraha, A. S., & Thahiruddin, M. (2020, June). Numerical Solution of Unsteady A12O3-Water Nanofluid Flow Past a Magnetic Porous Sliced Sphere. *Journal of Physics*, *1490*(1). 10.1088/1742-6596/1490/1/012070

Widodo, B., Siswono, G. O., & Imron, C. (2015). Viscoelastic Fluid Flow With the Presence of Magnetic Field Past a Porous Circular Cylinder. *International Journal of Mechanical And Production Engineering*, *3*(8), 123-126.

Widodo, B., Sulistyaningtyas, A., & Imron, C. (2015). The Effect of Prandtl Number and Viscosity Variable on Free Convection Boundary Layer Flowof a Viscoelastic Fluid Past an Elliptic Cylinder.

Yasin, S.H. M., Mohamed, M. K. A., Ismail, Z., Widodo, B., & Salleh, M. Z. (2021). Numerical Method Approach for Magnetohydrodynamic Radiative Ferrofluid Flows Over a Solid Sphere Surface. *Thermal Science*, *25*(2), 379-385. 10.2298/TSCI21S2379M

Zainal, N. A., Nazar, R., Naganthran, K., & Pop, I. (2020). MHD mixed convection stagnation point flow of a hybrid nanofluid past a vertical flat plate with convective boundary condition. *Chinese Journal of Physics*, *66*, 630-644. 10.1016/j.cjph.2020.03.022

Zaitun, Mahie, A. G., & Khaeruddin. (2021). A numerical model for pollutant distribution on a closed lagoon with inlet and outlet. *IOP Proceedings*, *763*(1), 012015. 10.1088/1755-1315/763/1/012015

Zaitun, Widodo, B., & Imron, C. (2024, January). Magnetohydrodynamic Nanofluid Flows Passing through a Smart Fabric under the Influence of Magnetic Field and Radiative Flux. *Journal of Advanced Research in Fluid Mechanics and Thermal Sciences*, *113*(1), 13-23. 10.37934/arfmts.113.1.1323